Performance Improvement of Artificial Neural Network Model in Short-term Forecasting of Wind Farm Power Output

Sergio Velázquez Medina and Ulises Portero Ajenjo

***Abstract*—Due to the low dispatchability of wind power, the massive integration of this energy source in power systems requires short-term and very short-term wind power output forecasting models to be as efficient and stable as possible. A study is conducted in the present paper of potential improvements to the performance of artificial neural network (ANN) models in terms of efficiency and stability. Generally, current ANN models have been developed by considering exclusively the meteorological information of the wind farm reference station, in addition to selecting a fixed number of time periods prior to the forecasting. In this respect, new ANN models are proposed in this paper, which are developed by: varying the number of prior 1-*h* periods (periods prior to the forecasting hour) chosen for the input layer parameters; and/or incorporating in the input layer data from a second weather station in addition to the wind farm reference station. It has been found that the model performance is always improved when data from a second weather station are incorporated. The mean absolute relative error (MARE) of the new models is reduced by up to 7.5%. Furthermore, the longer the forecasting horizon, the greater the degree of improvement.**

***Index Terms*—Artificial neural networks (ANN), wind power forecasting, model performance, wind power output.**

I. Introduction

A major impediment to the large-scale integration of wind power in electrical systems is the low dispatchability of this energy source. The effects of variations in wind speed, and hence wind power, are not only observed on a year-to-year or season-to-season scale, but also on a within-day scale [1]-[5]. A strategy that can be employed to improve wind energy integration in electric power systems is to optimize the performance of short-term forecasting models of wind power production. This strategy is the focus of the present study.

The direct consequences of the low dispatchability of wind power on electric power systems can be both technical and economic. Supply and demand adjustments in electric power systems are made 24-36 hours in advance. Any mismatches that might arise between supply and demand forecasting are subsequently corrected on the day itself [6]-[9]. As the result of imprecise forecasting, the mismatch correction entails additional costs for the electric power system [7], [10]. These extra costs are generally absorbed by the end user and/or electricity producer, with the latter thus burdened by an additional production cost.

Other strategies have been used to minimize the problem described above. One involves the direct estimation of the net energy demand of the electric power system, which can be understood as the difference between total demand and the energy generated by renewable sources. In [11], a model is proposed for direct forecasting of net energy demand which is validated with data from different electric power systems. Reference [12] compares a direct forecasting model of net energy demand with different indirect forecasting strategies.

In the electricity market, the matching of supply and demand is generally performed for 1 hour periods. For this reason, in an analysis of model forecasting performance, it is very important to evaluate the error for 1 hour periods, to study model performance for different forecasting horizons, and to evaluate the stability of the error in the time horizon in which the forecasting is made.

Numerous studies can be found in the literature on the development of short-term forecasting models. Different techniques and approaches have been analyzed and proposed. In most cases, good performances for specific forecasting horizons have been obtained. The techniques range from simple heuristics [13]-[17] to artificial intelligence [18]-[29]. This paper focuses on models which employ the technique of artificial neural networks (ANNs) to forecast wind power production [21], [22], [24]-[26], [28], [29].

In [29], the proposed forecasting model is developed based on the improvements of the Kriging interpolation

Manuscript received: November 16, 2018; accepted: December 13, 2019. Date of CrossCheck: December 13, 2019. Date of online publication: April 29, 2020.

This research was co-funded with ERDF funds, the INTERREG MAC 2014-2020 programme, within the ENERMAC project (No. MAC/1.1a/117). No funding sources had any influence on study design, collection, analysis, or interpretation of data, manuscript preparation, or the decision to submit for publication.

S. V. Medina (corresponding author) is with the Department of Electronics and Automatics Engineering, Universidad de Las Palmas de Gran Canaria, Campus de Tafira s/n, 35017 Las Palmas de Gran Canaria, Canary Islands, Spain (e-mail: sergio.velazquezmedina@ulpgc.es).

U. P. Ajenjo is with the School of Industrial and Civil Engineering, University of Las Palmas de Gran Canaria, Campus de Tafira s/n, 35017 Las Palmas de Gran Canaria, Canary Islands, Spain (e-mail: uportero@yahoo.es).

DOI: 10.35833/MPCE.2018.000792

method and empirical mode decomposition, which uses a new forecasting engine based on neural networks. To analyse the results, the mean absolute percentage error (MAPE), normalized mean absolute error (NMAE) and normalized root mean square error (NRMSE) metrics are used, calculated as the mean value in the forecasting horizons (24 hours and 6 hours). As in [29], models have been developed for different forecasting horizons [21], [22], [28]. However, an extensive analysis of the literature has found that the models developed to date only consider a specific and fixed number of prior 1-*h* periods (periods prior to the forecasting hour). It should also be noted that, in all the studies consulted, the meteorological data used as input layer parameters correspond exclusively to the reference weather station (WS) of the wind farm. In no case is the meteorological information used from additional WSs other than the reference WS of the wind farm. Finally, the metrics used to assess model performance in all these studies are obtained as the mean value of the forecasting time horizon. As previously stated, considering that the matching of supply and demand in the electricity market is performed for 1 hour periods, there is an additional interest in the study of the possible variation of the metrics within that time frame for each of the hourly periods.

This paper considers possible improvements, in terms of efficiency and stability, to the performance of ANN-based models for wind power forecasting. For this purpose, an analysis is made on the improvement of model performance of: varying the number of prior 1-*h* periods (periods prior to the forecasting hour) chosen for the ANN input layer parameters; and/or incorporating in the input layer data from a second WS in addition to the data from the wind farm reference station. The analysis is undertaken for a wide range of forecasting horizons. Based on the above, a total of up to 175 ANN models are generated, and the results are compared by applying the models to two actual wind farms located in the Canary Islands, Spain.

The aim of this paper is to make the following original contributions.

1) It investigates the improvement in the efficiency and stability of ANN models by varying the number of prior 1-*h* periods (periods prior to the forecasting hour and hereinafter referred to as *n*), chosen for incorporation of the input layer parameters.

2) It studies the improvement in ANN model performance of the additional incorporation in the input layer of meteorological data from WSs other than the wind farm reference station.

Both effects are analyzed for different forecasting horizons.

II. Methodology

Figure 1 shows the methodology for the implementation of different ANN models. It shows the combination of parameters which are considered for the input and output layer neurons in the generation process of different ANN models. The various parameters are defined as follows: t_i is the time instant based on which the forecasting is made; and V_{t_i}, D_{t_i} and P_{t_i} are the wind speed, wind direction and the wind farm power output at instant t_i, respectively.

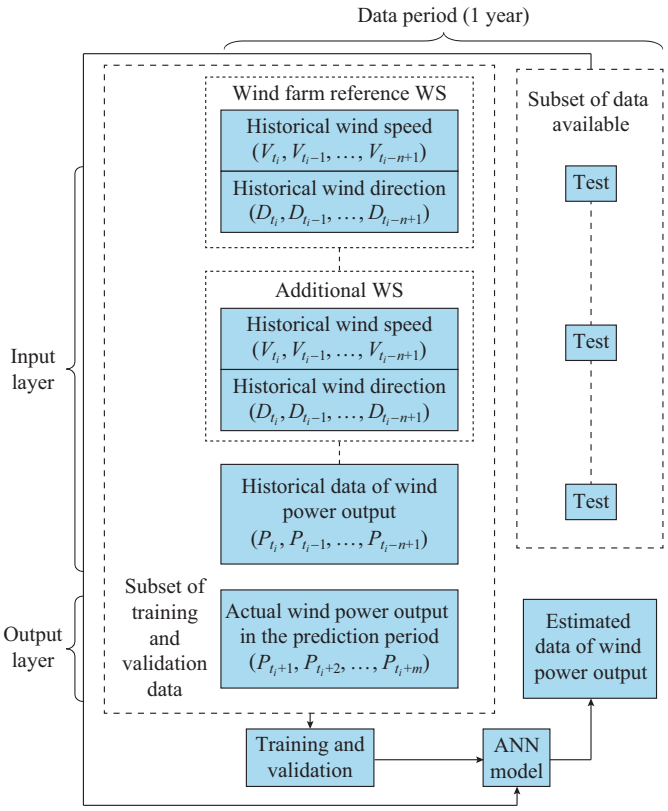

Fig. 1. Methodology to obtain forecasting models.

The following data are used in all the models: historical wind speed and direction data obtained from the wind farm reference WS, and historical power production data of the wind farm. In some models, which will be explained subsequently, the historical wind speed and direction data of a second WS are used in addition to the data of the wind farm reference station.

The output layer is composed of the power output values for different forecasting horizons.

The number of hours prior to the forecasting hour, *n*, and the length of the forecasting horizon that is being forecasted, *m*, are variable.

A. Architecture of ANN Employed

The ANNs used to generate the models are composed of three layers with feedforward connections. For this purpose, multi-layer perceptron (MLP) topologies have been used [30], [31]. In order not to increase the length of the training period excessively, a single layer of hidden neurons is used. This architecture has been shown to have the capacity to satisfactorily approximate any continuous transformation [30], [31]. Various prior tests have been carried out to choose the number of hidden neurons by varying the number of input signals. It is found that using more than 20 neurons merely increases the time required for model training and validation without improving the results. It is therefore decided to use a total of 20 neurons in the hidden layer.

The architectures are trained using the backpropagation algorithm with sigmoidal activation function [26], [27]. The Levenberg-Marquardt algorithm is used to minimize the mean square error committed in the learning process [30], [32].

To carry out the training and validation stages used to generate the model and the test stage of the network, the available annual data series for each parameter are divided into random and different subsets, as shown in Fig. 1. The proportion of data selected for each of the stages is 75%, 15% and 10%, respectively.

As can be seen in Fig. 1, the training and validation data subsets are used to generate the ANN model. The test data subset is used to evaluate the performance of the model.

The 10-fold cross-validation technique is used for the process of model generation and evaluation. The data subset of the test stage is used in each of the iterations. The error assigned to each model is the arithmetic mean of those obtained in the test stage for each of the iterations.

The various studies are performed using neural network tools available in the MATLAB software package.

B. Study Cases

1) Case A: comparison of efficiency and stability of different ANN models, which are obtained by varying the number of periods prior to the forecasting hour (n) chosen for incorporation of different parameters in the input layer.

The number of prior periods n and the number of forecasting horizon periods m are the studied variables. Different combinations of n and m generate different models whose performances will be analyzed. For Case A, both n and m are permitted to take the values 3, 6, 12, 24 and 36, i.e., five different models are generated for each forecasting horizon, and thus the total number of generated models is 25. This methodology is applied to the two wind farms.

To study the models in terms of the stability of forecasting, the results obtained for each of the periods within the forecasting horizon m are compared.

Figure 2 shows the structure of the neural network for this study case. The number of neurons of the output layer depends on the forecasting horizon, and will thus fluctuate between 3 and 36. For the input layer, the number of neurons will also vary depending on the value of n, from 9 ($n=3$) to 108 ($n=36$).

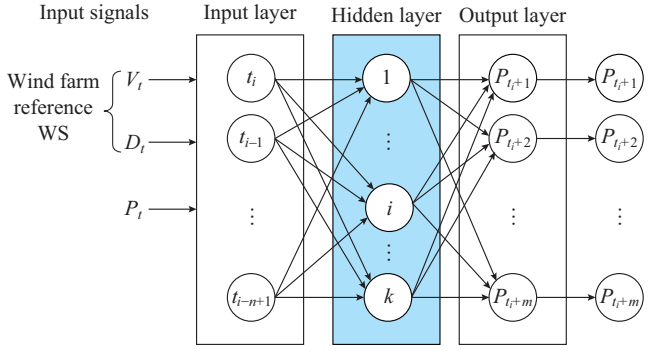

Fig. 2. Schematic representation of neural network for generation of forecasting models in Case A.

2) Case B: comparison of performance of ANN models when additionally incorporating in the input layer the data from a second WS other than the reference station of wind farm. For Case B, both n and m could take the same values as indicated for Case A.

Figure 3 shows the structure of the neural network for the generation of models in Case B.

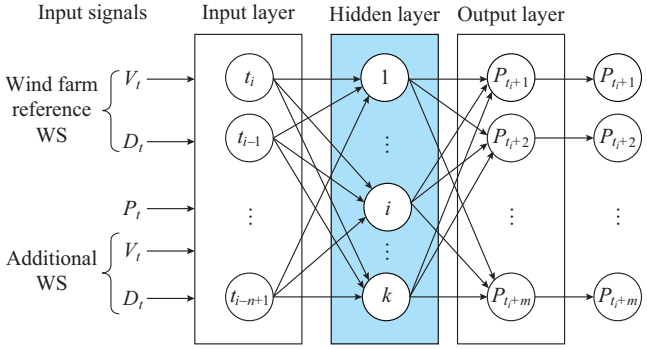

Fig. 3. Schematic representation of neural network for generation of forecasting models in Case B.

In Case B, the input layer of the ANN incorporates the data from a second WS in addition to that of the reference WS of the wind farm. To generate different models, the data of the reference WS of each wind farm (WS1 and WS9) are combined with the data of each of the seven other WSs, WS2 to WS8 (Table I). Therefore, for Case B, 175 different models are generated (25×7). After applying these models to each wind farm, their results are compared.

TABLE I
INFORMATION OF WSS

Code	Height above ground level (m)	Latitude (north)	Longitude (west)	Altitude (m)
WS1	40	27°54′08″	15°23′17″	16
WS2	10	27°51′36″	15°23′13″	3
WS3	10	28°27′10″	13°51′54″	24
WS4	10	28°57′07″	13°36′00″	10
WS5	13	28°01′36″	15°23′16″	5
WS6	10	28°07′30″	15°40′37″	472
WS7	10	27°56′08″	15°25′24″	186
WS8	10	28°02′35″	16°34′16″	51
WS9	40	29°05′47″	13°30′21″	457

The number of neurons in the input layer also varies, depending on the value of n, from 15 ($n=3$) to 180 ($n=36$).

The variation in the number of output layer neurons is the same as in Case A.

C. Metrics Used to Compare Different Models

To compare the performance of the different models generated for Cases A and B, metrics (1) and (2) are used:

$$MARE=\frac{1}{m}\sum_{j=1}^{m}\frac{1}{T-r}\sum_{i=1}^{T-r}\frac{\left|P_{ji}-\hat{P}_{ji}\right|}{P_{ji}}=\frac{1}{m}\sum_{j=1}^{m}MARE_j \quad (1)$$

$$R=\frac{1}{m}\sum_{j=1}^{m}\frac{\sum_{i=1}^{T-r}\left(P_{ji}-\bar{P}_j\right)\left(\hat{P}_{ji}-\bar{\hat{P}}_j\right)}{\sqrt{\left[\sum_{i=1}^{T-r}\left(P_{ji}-\bar{P}_j\right)^2\right]\left[\sum_{i=1}^{T-r}\left(\hat{P}_{ji}-\bar{\hat{P}}_j\right)^2\right]}}=\frac{1}{m}\sum_{j=1}^{m}R_j \quad (2)$$

where *MARE* is the mean absolute relative error for the forecasting horizon; T is the number of data in the test stage (see Fig. 1); $r=T-m-n$; $MARE_j$ is the mean absolute relative error for the forecasting period j; P_j and $\hat{P}_j$ are the actual and estimated wind farm power outputs in the forecasting period j, respectively; $\bar{P}_j$ and $\bar{\hat{P}}_j$ are the mean values of P_j and $\hat{P}_j$, respectively; R is the mean value of the Pearson correlation coefficient between the estimated and actual wind farm power outputs for the forecasting horizon; and R_j is the mean Pearson correlation coefficient between the estimated and actual wind power outputs for the forecasting period j.

III. Materials

The meteorological data (wind speed and direction) recorded by nine WSs located in four of the seven islands of the Canary Archipelago (Table I) are used in this paper. The mean hourly wind speed and direction data from 2008 are used in all cases. The heights of the WSs are expressed in metres above ground level.

To validate and compare the results obtained with the different models, the information corresponding to two wind farms located on two of the seven islands of the Canary Archipelago is used. Tables II and III show the geographic coordinates of the wind turbines (WT1-WT9) of the two wind farms (WF1 and WF2). The hourly wind power output data for 2008 are used for this study.

TABLE II
GEOGRAPHIC COORDINATES OF WIND TURBINES IN WF1

Code	x (m)	y (m)	z (m)
WF1-WT1	461764	3086314	3
WF1-WT2	461839	3086301	1
WF1-WT3	461681	3086067	5
WF1-WT4	461753	3086038	2

TABLE III
GEOGRAPHIC COORDINATES OF WIND TURBINES IN WF2

Code	x (m)	y (m)	z (m)
WF2-WT1	645043	3219819	486
WF2-WT2	645147	3219752	478
WF2-WT3	645186	3219638	473
WF2-WT4	645264	3219548	464
WF2-WT5	645333	3219462	456
WF2-WT6	645403	3219369	448
WF2-WT7	645406	3219213	440
WF2-WT8	645554	3219194	425
WF2-WT9	645664	3219133	405

Stations WS1 and WS9 in Table I are the reference WSs of wind farms WF1 and WF2, respectively. The data of WS1 and WS9 and the wind power production values are provided by the respective owners of the wind farms. The data from the seven additional WSs are provided by the Canary Islands Technological Institute (Spanish initials: ITC) and Spain's Sate Meteorological Agency (Spanish initials: AEMET).

Table IV shows the results obtained for the coefficients of linear correlation (3) between the mean hourly wind speeds of the different WSs.

$$CC=\frac{\sum_{i=1}^{NG}\left(V_i-\bar{V}\right)\left(V_i'-\bar{V}'\right)}{\sqrt{\sum_{i=1}^{NG}\left(V_i-\bar{V}\right)^2}\sqrt{\sum_{i=1}^{NG}\left(V_i'-\bar{V}'\right)^2}} \quad (3)$$

where CC is the Pearson correlation coefficient between the wind speeds of two WSs; V_i and V_i' are the speeds at instant i of the two WSs subject to correlation; $\bar{V}$ and $\bar{V}'$ are the mean values of V_i and V_i', respectively; and NG is the total number of data of the series. In this case, as a series of hourly data equivalent to one year is available, $NG=8760$.

TABLE IV
COEFFICIENT OF LINEAR CORRELATION BETWEEN WIND SPEEDS OF DIFFERENT WSS IN 2008

Code	Coefficient of linear correlation								
	WS1	WS2	WS3	WS4	WS5	WS6	WS7	WS8	WS9
WS1	1.00	0.84	0.27	0.34	0.74	0.73	0.77	0.50	0.51
WS2	0.81	1.00	0.19	0.25	0.79	0.74	0.87	0.44	0.54
WS3	0.27	0.19	1.00	0.70	0.16	0.16	0.18	0.16	0.11
WS4	0.34	0.25	0.70	1.00	0.20	0.21	0.22	0.20	0.11
WS5	0.74	0.79	0.16	0.20	1.00	0.49	0.78	0.21	0.44
WS6	0.73	0.74	0.16	0.21	0.49	1.00	0.61	0.62	0.54
WS7	0.77	0.87	0.18	0.22	0.78	0.61	1.00	0.39	0.46
WS8	0.50	0.44	0.16	0.20	0.21	0.62	0.39	1.00	0.35
WS9	0.51	0.54	0.11	0.11	0.44	0.54	0.46	0.35	1.00

IV. Results and Discussion

The discussion focuses on the two cases proposed in the methodology. For the various figures corresponding to the results, $t-3$ indicates that 2 periods prior to the forecasting period are chosen in addition to the forecasting period (t_i, t_i-1, t_i-2), and $t+3$ indicates a forecasting horizon of 3 periods (t_i+1, t_i+2, t_i+3) starting from the period when the forecasting is made. The same is true for all combinations.

A. Discussion of Results for Case A

Figures 4 and 5 show the results for the *MARE* and R metrics for the 25 generated models. In all practical cases, the *MARE* and R values improve as n increases. The only exception is for case $t-36$ compared to $t-24$, where the improvement is minimal or not observed. Besides, the degree of improvement increases as m increases ($t+12$, $t+24$ and $t+36$).

For the forecasting horizons $t+12$, $t+24$, $t+36$, the maximum improvements obtained for *MARE* between the values for $n=3$ and $n=36$ are 13.3%, 11.2% and 10%, respectively. For the same cases but for R, the corresponding improvements are 7.9%, 8.9% and 9.2%, respectively.

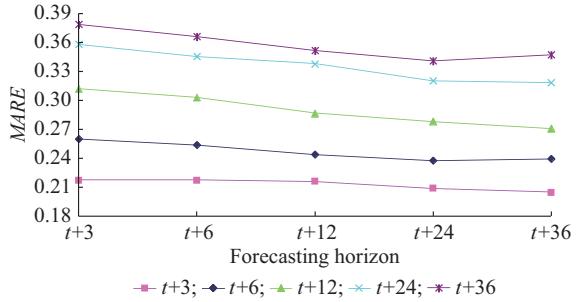

Fig. 4. *MARE* results in Case A.

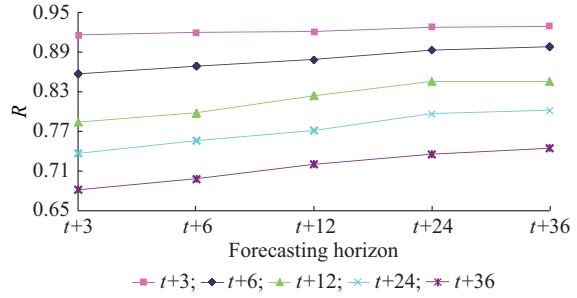

Fig. 5. *R* results in Case A.

To study the forecasting stability, an analysis has been made for the case of forecasting horizon $t+24$, in which the number of forecasting periods is significant. Figure 6 shows the results of the variation of the relative error in different forecasting periods, $MARE_j$, for this specific case differentiated according to n. It can be seen that the relative error stabilizes earlier as n increases.

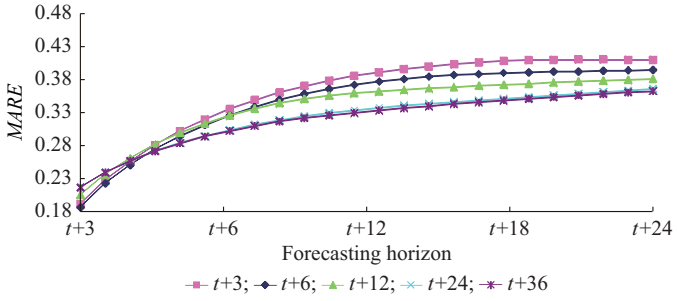

Fig. 6. *MARE* variation of different forecasting periods: case of a forecasting horizon $t+24$.

Figure 7 shows that the forecasting stability is analyzed for all the forecasting horizons.

This analysis is made on the basis of the standard deviation of relative error in the forecasting horizon:

$$SDV = \sqrt{\frac{1}{m-1}\sum_{j=1}^{m}\left(MARE_j - MARE\right)^2} \tag{4}$$

where *SDV* is the mean standard deviation of *MARE* for a forecasting time horizon m.

It can be seen in Fig. 7 that for all the forecasting horizons, the *SDV*/*MARE* value decreases significantly as the number of prior hours n increases. This significant improvement in the stability of models is observed even for the lowest forecasting horizons. Only for the particular case of forecasting horizon $t+3$ and when the horizon passes from $t-24$ to $t-36$, no improvement is observed.

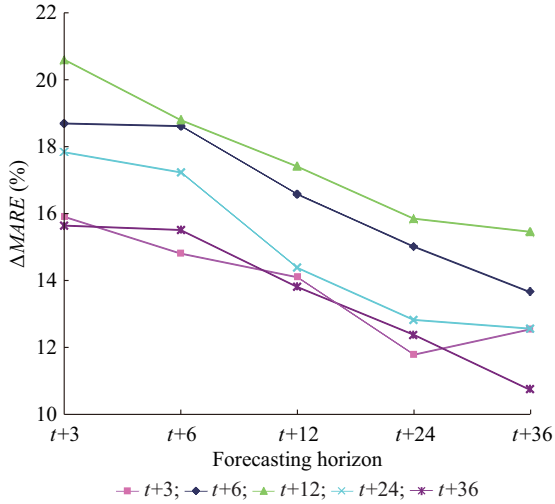

Fig. 7. Stability of relative error *SDV* in forecasting horizon.

As an example, we will now proceed to analyze the cases of the forecasting models $t+12$ and $t+24$. To date, in the ANN models studied in the literature, the number of prior periods n chosen to generate the models has always been fixed. Assume that n is chosen as 12 for a standard model. As shown in Fig. 4, the *MARE* value is 0.2866 for the $t+12$ model and 0.3382 for the $t+24$ model, respectively. As shown in Fig. 7, the corresponding values for the stability of the relative error are 17.4% and 14.4%, respectively. According to the analysis made with Case A, the performance of these models can be improved by choosing a higher value of n. As shown in Fig. 4, if $n=24$, the *MARE* values decrease to 0.2783 and 0.3206, respectively. Similarly, as shown in Fig. 7, for $n=24$, the stability of the relative error in the forecasting improves to 15.8% and 12.8%, respectively.

B. Discussion of Results for Case B

For Case B, the *MARE* and *R* results of this case with two WSs ($MARE_B$, R_B), are compared with those of Case A with one WS ($MARE_A$, R_A), as shown in (5) and (6).

$$\Delta MARE = \frac{1}{7}\sum_{p=1}^{7}\frac{MARE_B - MARE_A}{MARE_A}\times 100\% \tag{5}$$

$$\Delta R = \frac{1}{7}\sum_{p=1}^{7}\frac{R_B - R_A}{R_A}\times 100\% \tag{6}$$

It can be seen in Figs. 8 and 9 that all the models generated for Case B achieve an additional improvement in performance compared to that for Case A. This additional improvement is in relation to the developed ANN models, where exclusive data is used from a single WS. It can also be observed that, in general, the degree of improvement increases as m increases. This degree of improvement slows down for forecasting horizons longer than 24 hours.

The maximum additional improvements in model performance are seen in forecasting horizons $t+24$ and $t+36$ (7.5% and 5.5% for *MARE* and 3.7% and 5.4% for *R*, respectively). Even for the shortest forecasting horizons, $t+3$

and $t+6$, the maximum improvements in the *MARE* metric are significant (3% and 4.9%, respectively).

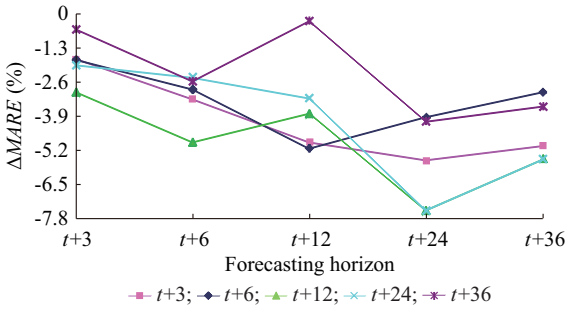

Fig. 8. Comparison of *MARE* results for Cases A and B.

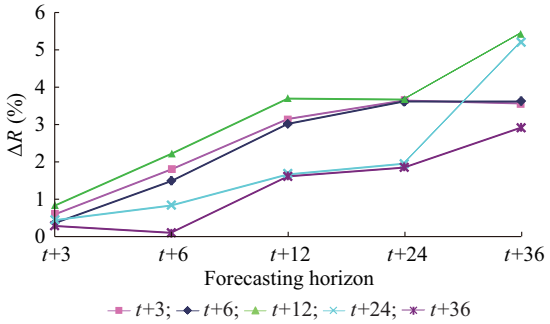

Fig. 9. Comparison of *R* results for Cases A and B.

Continuing with the specific example proposed in the analysis of results for Case A (using models $t+12$ and $t+24$), Fig. 10 shows the additional improvements in performance that can be obtained through the incorporation in the input layer of data from the second WS (Case B).

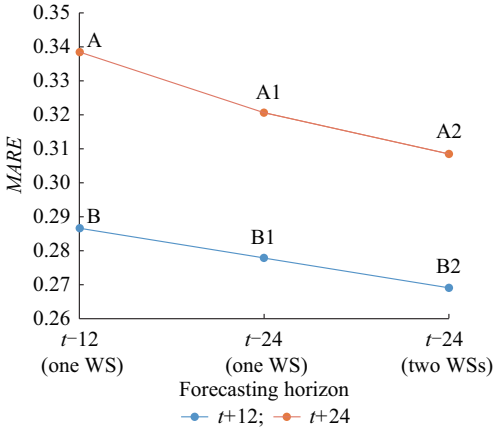

Fig. 10. Improvements in error for two specific models due to implementation of Cases A and B.

Points A and B represent the error obtained when using a fixed n of 12 and only data from the reference WS of the wind farm. Points A1 and B1 represent the improvements obtained in the error in Case A when n is increased to 24. Points A2 and B2 represent the additional improvements obtained in the error in Case B when the data from the second WS are incorporated in the input layer of the ANN. For the two specific examples, the overall improvements obtained by combining Cases A and B equal to 8.78% and 6.04%, respectively.

V. Conclusion

A series of conclusions can be drawn from the results of this study with respect to possible improvements in the performance of ANN models for the short-term forecasting of wind power output.

The performance of the new ANN models generated for each forecasting horizon is improved with the increase in the number of prior 1-h periods prior to the forecasting hour, which is chosen for the incorporation of the input layer parameters. For the forecasting horizons $t+12$, $t+24$ and $t+36$, the maximum improvements obtained for *MARE* are 13.3%, 11.2% and 10%, respectively; and for *R*, the corresponding improvements are 7.9%, 8.9% and 9.2%, respectively.

The stability of the mean relative error is also studied for the different forecasting periods and for each forecasting horizon m. As n increases, the stability of the error in the forecasting is significantly improved for all forecasting horizons.

Additionally, in all the new models, the incorporation in the input layer of ANN of meteorological data from a second WS also helps improve the performance of the traditional models with data from the reference station of the wind farm. In general, the degree of improvement in model performance increases with m, attaining improvements in *MARE* and *R* of up to 7.5% and 5.4%, respectively.

References

[1] C. G. Justus, K. Mani, and A. S. Mikhail, "Interannual and month-to-month variations of wind speed," *Journal of Applied Meteorology*, vol. 18, no. 7, pp. 913-920, Jul. 1979.

[2] R. Baker, S. N. Walker, and J. E. Wade, "Annual and seasonal variations in mean wind speed and wind turbine energy production," *Solar Energy*, vol. 45, no. 5, pp. 285-289, Jan. 1990.

[3] K. Klink, "Trends and interannual variability of wind speed distributions in Minnesota," *Journal of Climate*, vol. 15, no. 22, pp. 3311-3317, Nov. 2002.

[4] T. Burton, *Wind Energy Handbook*, 2nd ed. New York: John Wiley & Sons, 2011.

[5] L. Landberg, L. Myllerup, O. Rathmann *et al.*, "Wind resource estimation – an overview", *Wind Energy*, vol. 6, no. 3, pp. 261-271, Jul. 2003.

[6] A. Aziz, A. M. Than, and A. Stojcevski, "Issues and mitigations of wind energy penetrated network: Australian network case study," *Journal of Modern Power Systems and Clean Energy*, vol. 6, no. 6, pp. 1141-1157, Nov. 2018.

[7] A. Basit, A. D. Hansen, P. E. Sørensen *et al.*, "Real-time impact of power balancing on power system operation with large scale integration of wind power," *Journal of Modern Power Systems and Clean Energy*, vol. 5, no. 2, pp. 202-210, Mar. 2017.

[8] T. Mahmoud, Z. Y. Dong, and J. Ma, "Advanced method for short-term wind power prediction with multiple observation points using extreme learning machines," *The Journal of Engineering*, vol. 2018, no. 1, pp. 29.38, Mar. 2018.

[9] P. Du, H. Hui, and N. Lu, "Procurement of regulation services for a grid with high-penetration wind generation resources: a case study of ERCOT," *IET Generation, Transmission and Distribution*, vol. 10, no. 16, pp. 4085-4093, Dec. 2016.

[10] A. Basit, A. D. Hansen, M. Altin *et al.*, "Compensating active power imbalances in power system with large-scale wind power penetration," *Journal of Modern Power Systems and Clean Energy*, vol. 4, no. 2, pp. 229-237, Mar. 2016.

[11] O. Abedinia and N. Amjady, "Net demand prediction for power systems by a new neural network-based forecasting engine," *Complexity*, vol. 21, pp. 296-308, Jul. 2016.

[12] M. Bagheri, O. Abedinia, M. Salary *et al.*, "Direct and indirect predic-

tion of net demand in power systems based on syntactic forecast engine," in *Proceedings of IEEE International Conference on Environment and Electrical Engineering*, Palermo, Italy, Jun. 2018, pp. 1-6.
[13] Y. Jiang, X. Chen, K. Yu *et al*., "Short-term wind power forecasting using hybrid method based on enhanced boosting algorithm," *Journal of Modern Power Systems and Clean Energy*, vol. 5, no. 1, pp. 126-133, Jan. 2017.
[14] H. Chen, F. Li, and Y. Wang, "Wind power forecasting based on outlier smooth transition autoregressive GARCH model," *Journal of Modern Power Systems and Clean Energy*, vol. 6, no. 3, pp. 532-539, May 2018.
[15] M. Xu, Z. Lu, Y. Qiao *et al*., "Modelling of wind power forecasting errors based on kernel recursive least-squares method," *Journal of Modern Power Systems and Clean Energy*, vol. 5, no. 5, pp. 735-745, Sept. 2017.
[16] D. Kim and J. Hur, "Short-term probabilistic forecasting of wind energy resources using the enhanced ensemble method," *Energy*, vol. 157, pp. 211-226, Aug. 2018.
[17] N. Huang, E. Xing, G. Cai *et al*., "Short-term wind speed forecasting based on low redundancy feature selection," *Energies*, vol. 11, no. 7, 1638, Jul. 2018.
[18] T. Liu, S. Liu, J. Heng *et al*., "A new hybrid approach for wind speed forecasting applying support vector machine with ensemble empirical mode decomposition and cuckoo search algorithm," *Applied Sciences*, vol. 8, no. 10, pp. 1754, Oct. 2018.
[19] O. Abedinia, D. Raisz, and N. Amjady, "Effective prediction model for Hungarian small-scale solar power output," *IET Renewable Power Generation*, vol. 11, no. 13, pp. 1648-1658, Nov. 2017.
[20] Y. Zhang, K. Liu, L. Qin *et al*., "Deterministic and probabilistic interval prediction for short-term wind power generation based on variational mode decomposition and machine learning methods," *Energy Conversion and Management*, vol. 112, pp. 208-219, Jan. 2016.
[21] A. Zameer, J. Arshad, A. Khan *et al*., "Intelligent and robust prediction of short term wind power using genetic programming based ensemble of neural networks," *Energy Conversion and Management*, vol. 134, pp. 361-372, Feb. 2017.
[22] M. Felder, F. Sehnke, K. Ohnmeiß *et al*., "Probabilistic short term wind power forecasts using deep neural networks with discrete target classes," *Advances in Geosciences*, vol. 45, pp. 13-17, Jul. 2018.
[23] N. Ullah, A. Zameer, A. Khan *et al*., "Machine learning based short term wind power prediction using a hybrid learning model," *Computers and Electrical Engineering*, vol. 45, pp. 122-133, Jul. 2015.
[24] M. Morina, F. Grimaccia, S. Leva *et al*., "Hybrid weather-based ANN for forecasting the production of a real wind power plant," in *Proceedings of 2016 International Joint Conference on Neural Networks (IJCNN)*, Vancouver, Canada, Jul. 2016, pp. 1-6.
[25] P. Mandal, H. Zareipour, and W. D. Rosehart, "Forecasting aggregated wind power production of multiple wind farms using hybrid wavelet-PSO-NNs," *International Journal of Energy Research*, vol. 38, no. 13, pp. 1654-1666, Feb. 2014.
[26] G. Zhang, L. Zhang, and T. Xie, "Prediction of short-term wind power in wind power plant based on BP-ANN," in *Proceedings of IEEE Advanced Information Management, Communicates, Electronic and Automation Control Conference*, Xi'an, China, Oct. 2016, pp. 75-79.
[27] A. Tascikaraoglu and M. Uzunoglu, "A review of combined approaches for prediction of short-term wind speed and power," *Renewable and Sustainable Energy Reviews*, vol. 34, pp. 243-254, Jun. 2014.
[28] D. Lee and R. Baldick, "Short-term wind power ensemble prediction based on Gaussian processes and neural networks," *IEEE Transactions on Smart Grid*, vol. 5, no. 1, pp. 501-510, Jan. 2014.
[29] N. Amjady and O. Abedinia, "Short term wind power prediction based on improved Kriging interpolation, empirical mode decomposition, and closed-loop forecasting engine," *Sustainability*, vol. 9, no. 11, pp. 2104, Nov. 2017.
[30] J. C. Principe, N. R. Euliano, and W. C. Lefebvre, *Neural and Adaptive Systems: Fundamentals Through Simulations*, 1st ed. New York: John Wiley & Sons, 2000.
[31] T. Masters, *Practical Neural Network Recipes in C++*, 1st ed. California: Morgan Kaufmann Publishers, 1993.
[32] N. R. Draper and H. Smith, *Applied Regression Analysis*, 3rd ed. New York: John Wiley & Sons, 1998.

Sergio Velázquez Medina received the Master's and Ph.D. degrees in 1997 and 2011, respectively, both in industrial engineering from the University of Las Palmas de Gran Canaria (ULPGC), Canary Islands, Spain. From 1997 to 2005, he worked with the Canary Islands Technological Institute (ITC), an research & development (R&D) institution run by the Canary Islands Government, as head of the wind energy exploitation area. Since 2006, he has been a professor with the Department of Electronics and Automatics Engineering in the ULPGC and a member of the Group for Research on Renewable Energy Systems (GRRES). His research interests include modeling of renewable resources and integration of non-manageable renewable installations in electrical systems.

Ulises Portero Ajenjo received the Master's degree in 2005, and the Ph.D. degree in 2016, both in engineering in industrial organization, from the University of Las Palmas de Gran Canaria (ULPGC), Canary Islands, Spain. In 2002 and 2003, he worked in the Computer and Systems Department of the Canary Islands Technological Institute, Canary Islands, Spain. Since 2005, he has been working in the IT Department of the Municipal Government of Las Palmas de Gran Canaria, Canary Islands, Spain. Since 2016, he has been collaborating with the School of Industrial and Civil Engineering of ULPGC in R&D projects. His research interests include the development of renewable energy system models using artificial intelligence techniques.